ACTA SCIENTIFIC DENTAL SCIENCES (ISSN: 2581-4893)

Volume 2 Issue 12 December 2018

Research Article

Validation of a Numerical Model Representative of an Oral Rehabilitation with Short Implants

J Ferreira*

Faculty of Engineering of the University of Porto (FEUP), Institute of Mechanical Engineering and Industrial Management (INEGI), Porto, Portugal

***Corresponding Author:** J Ferreira, Faculty of Engineering of the University of Porto (FEUP), Institute of Mechanical Engineering and Industrial Management (INEGI), Porto, Portugal.

Received: September 04, 2018; **Published:** November 02, 2018

Abstract

A numerical model representative of an oral rehabilitation with short implants was subjected to experimental validation. The electronic speckle pattern interferometry (ESPI) was chosen as experimental technique. The numerical and the experimental models exhibited similar behavior allowing for the intended validation.

Keywords: Medical Images; Numerical Model; Interferometry; Displacement

Introduction

Mandibular rehabilitations, with short implants, are still subject of debate due to concerns related with the disproportional crown-to-implant ratio [1,2] and the possibility of the bending forces, resulting from the horizontal component of the masticatory loads, cause shear stresses with detrimental effects on bone and prosthetic components [2,3]. These concerns are aggravated by the inexistence of a periodontal ligament on dental implants, what reduces the tactile perception and may result in occlusal overloads [4,5]. The assessment of the mechanical performance of these type of rehabilitations could benefit from the use of a finite element analysis (FEA), method widely used in dental implants to predict the behavior of biological structures and prosthetic solutions [6,7]. This method allows to predict the behavior of multiple combinations of critical factors and may precede clinical trials. However, the FEA results are dependent on the calculation conditions. Despite the efforts to resemble the real conditions, differences will subsist. Geometry simplifications, often necessary to reduce calculation time or materials' properties, frequently imported from bibliography, are examples of how the similitude between the numerical and the real models may be affected [8, 9]. Thus, it is important to experimentally validate the numerical model in order to allow trustworthy conclusions. Due to the differences existent between the numerical and the experimental model, it is worth to underline that the validation process consists more on finding a similitude of behavior and tendencies than on a quantitative exactitude of measurements [10,11].

The classical validation method, using strain gauges in combination with a load appliance, faces some potential problems. The model dimensions may preclude the placement of strain gauges on important locations for stress/strain assessment on implant rehabilitations. Strain gauges only provide point measurements on the model's surface, without giving information on stress/strain variations at the whole inspection area [12] and making hard to accurately determine their corresponding position on the numerical model [13].

The use of optical techniques may overcome such problems. The electronic speckle pattern interferometry (ESPI), non-destructive, with no contact with the object, and providing whole surface information on displacement distribution [8,14], is a method is based on the interferometry between holographic recordings to assess the displacements suffered by a loaded surface with submicrometric resolution. This interference is visually translated by a fringe pattern that represents the displacement field of the surface under study [14,15]. This is an extremely accurate method, able to measure displacements of half the wavelength of the coherent light used [15] which also makes ESPI extremely sensitive to environment disturbances, what advises a very controlled experimental set up.

The possibility of using optical methods to validate numerical models is documented on the bibliography [13,14]. However, it did not come to the author's knowledge any study where an oral rehabilitation FEA model was validated with ESPI.

Materials and Methods

Numerical model

With the consent of the patients, 2D and 3D medical images obtained from computational tomographys (Figure 1a, 1b, 2a, 2b and 2c), where analyzed and served as the base to design a simplified model, representative of a partial posterior screw-retained mandible rehabilitation, with two short-implants (Figure 3). Some measurements were carried out, such as the distance from the mandible lower border to the molar cusps, the mandible width, the diameter of the mandibular canal, the distance from the lowest point of the mandibular canal to the mandibular lower border and the cortical bone width. From the obtained measurements for each parameter, an average was calculated and used in the modeling process which also included the simplified design of external hexagon short dental implants, prosthetic screws, cortical and trabecular bone. On Abaqus® software (Dassault Systèmes SA, Vélizy, France), the geometrical model was transformed into a numerical model (Figure 4). This process consisted on the assignment of materials and the correspondent properties, as well as the definition of contact properties between the different parts (Table 1). On the bone parts (cortical and trabecular), epoxy resin properties were considered once, for the model materialization, it has similar properties to the human bone. Resin and implants were merged to simulate osseointegration, maintaining the properties of each material. The load was defined as a surface traction, applying a load of 1 N divided for 3 circumferential areas with a 0.45 mm radius, which resulted on a pressure of 0.529 Nmm2 on each area. A mesh sensitivity study was performed [16], considering partitions of the different parts with more refined meshes where higher stresses were observed, resulting on the number of elements depicted on the table 2. After meshing, on the prosthetic framework a set of nodes was defined to posteriorly be used on the displacement's measurements. An encastre boundary condition was defined on the lower face of the resin.

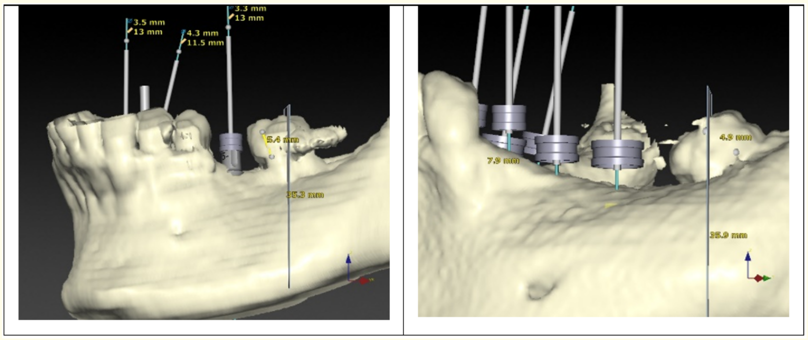

Figure 1a and 1b: Three-dimensional medical image obtained from a computerized tomography used to obtain the model dimensions.

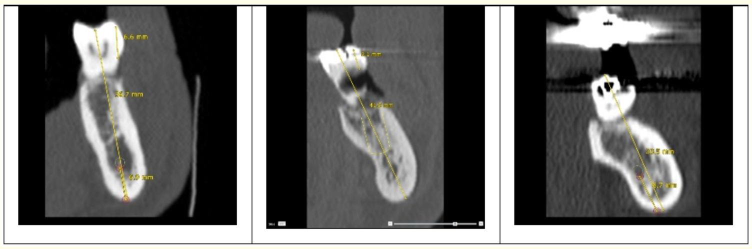

Figure 2a, 2b and 2c: Two-dimensional medical image obtained from a computerized tomography used to obtain the model dimensions.

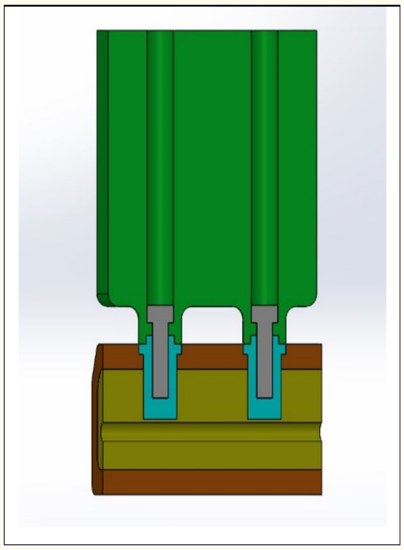

Figure 3: Cut of the model designed on SolidWorks®, where it is possible to observe a prosthetic framework with two screw channels (green), two prosthetic screws (grey), two short implants (blue) and cortical (brown) and trabecular bone (dark yellow).

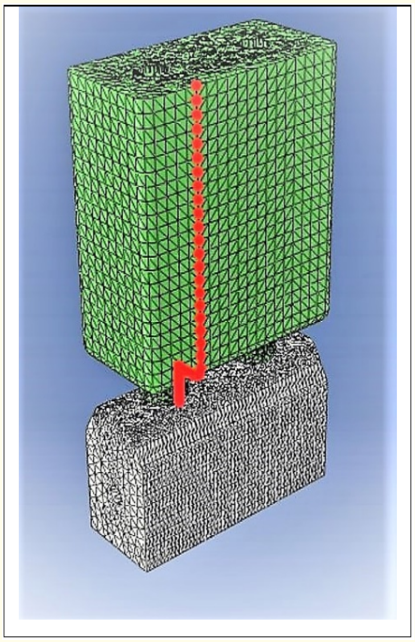

Figure 4: External view of the numerical model exhibiting the mesh and the set of nodes used to compare the displacements.

Parts	Material	Young's Modulus (MPa)	Poisson coefficient	Yield strength (MPa)
Resin	Resin	20 000	0.363	45
Implants and implant screws	Ti6Al4V alloy	120 000	0.33	795
Prosthetic framework	Co-Cr alloy	194 000	0.30	659
Coefficient of friction for Ti6Al4V alloy with Co-Cr alloy				0.15
Coefficient of friction for Ti6Al4V alloy with itself				0.43

Table 1: Materials, elastic properties and friction coefficients elected for each part of the model [17-23].

Model's part	Element size on partitions (mm)	Number of elements	Number of nodes
Resin	0.2	77868	116821
Implants	0.2	32148	48822
Implant screws	0.6	550	1003
Prost framework	0.15	368027	536754

Table 2: Average element size (C3D10, a quadratic tetrahedral element), number of elements and nodes obtained after meshing separately each part of the model.

Specimen preparation

The model materialization was performed using implant dummies and prosthetic screws obtained from Nobel Biocare (Nobel Biocare AB, Gothenburg, Sweden), epoxy resin developed and characterized at INEGI (institute of mechanical engineering and industrial management, Porto, Portugal), where the prosthetic frameworks were also milled in a cobalt-chrome alloy. A resin base was modelled in order to allow a load direction with the same characteristics as the mathematical model. Three samples (U1, U2 and U3) were obtained and submitted to ESPI measurements.

ESPI

An experimental setup was assembled on the top of an optical table to maximize stability. A loading rig was prepared to hold the samples and apply the testing loads. A Diode-Pumped Solid State Coherent Verdi laser, emitting up to 2W at 532 nm was used as light source and the camera JAI model CV-M2 CCD 1608hx 1216v pixels, was used to record interferometry images. Data was processed by the software developed in Matlab to compute the phase distribution using phase modulation techniques. The experimental set up can be observed on the figure 5.

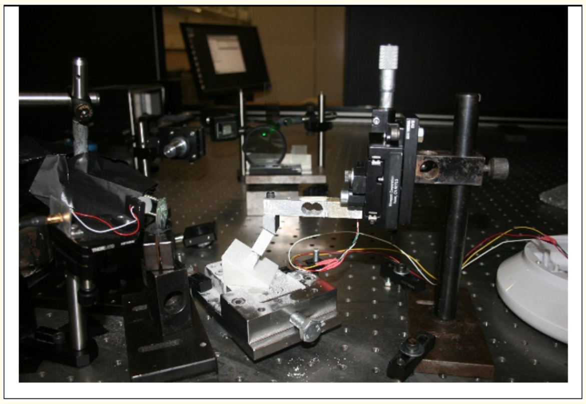

Figure 5: Experimental set up highlighting the specimen mounting device and its positioning.

Due to the high sensitivity of ESPI, the load intensity is difficult to control in a stable way. So, the most accurate form to execute the test is to impose a displacement and measure the correspondent reaction force, what was achieved by the use of a screw threaded in a load cell. In this experiment, the three samples were subjected to four displacements which generated different reaction forces as shown on table 3.

	Reaction force (N)			
Sample 1	1.66	2.00	2.36	3.43
Sample 2	1.73	1.96	2.45	3.92
Sample 3	1.42	1.98	2.48	3.89

Table 3: Reaction forces obtained for each tested sample.

Results

Analyzing the results from FEA, the maximum displacement obtained was 2.41 μm, on the top of the prosthetic framework and 0.139 μm were measured on the bottom of the connector as the lowest displacement. The results extracted from the set of nodes allowed the construction of a graphic (Figure 6) where it is possible to observe a first segment with a small discontinuity with a second segment. This difference is related with the different geometries of the connector and the framework body. This data indicates that the prosthetic framework essentially suffers a rotation rather than a deformation, which center is impossible to identify with the available data. The results obtained could also be presented in the form of an image where a colour codification represents the different obtained displacements (Figure 7).

Analyzing data obtained from ESPI experiments and converting to a graphic mode (Figure 8), it is also possible to observe a linear behavior correspondent to a rotation. When different displacements are applied to the samples they show a similar behavior. It can be observed that, an increasing on the applied displacement resulted in an increased displacement of the prosthetic framework. This tendency is not observed only on sample U2 1,96N. It can also be seen that the graphic line becomes more perfect for higher reaction forces, as a possible result of overcoming an accommodation phenomenon.

Finally, the initial part of the graphics, for a horizontal coordinate around 20, shows a different behavior correspondent to the different geometry of the framework connector. The major displacements were measured, for each sample and each reaction force, on the top of the prosthetic framework. The lowest displacements were obtained on the connector, as revealed on table 4, showing the same tendency as the FEA.

One of the fringe patterns recorded can be observed on figure 9a (sample U3; 2.48 N). Its transduction into a color code (Figure 9b) results in an image similar to the obtained on FEA, what facilitates the comparison between both models' results.

The coordinates attributed by the software ISTRA from Ettermyer to the ESPI results did not match the FEA coordinates. Likewise, the force applied to the numerical model (1N) and the reaction forces measured on the ESPI were different. For these reasons, the results were formatted so that the highest abscissa coordinate (25 mm) could match both studies and the reaction forces corresponded to 1N, to allow a direct comparison of the results. For that propose, to avoid possible effects of accommodation, the highest reaction forces of each sample were elected, and an arithmetical average was calculated. The result is depicted on the figure 10, where a maximum displacement of 1,618 μm can be found and a comparison with the FEA results is shown.

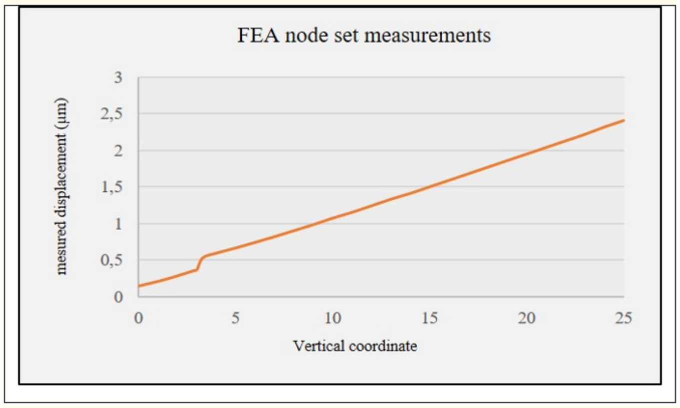

Figure 6: Displacement computed, on FEA, on the node set.

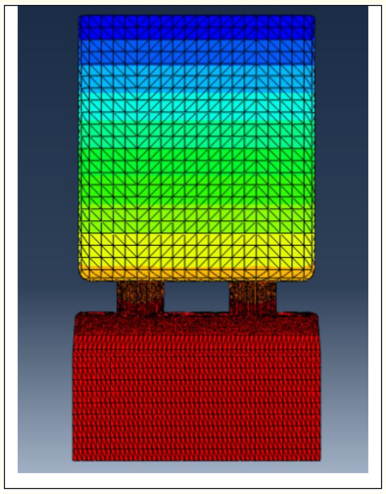

Figure 7: Displacements obtained with the numerical model exposed with recourse to an image colour code.

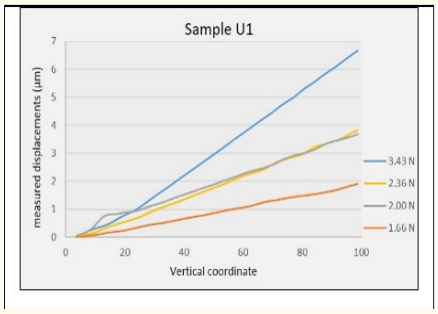

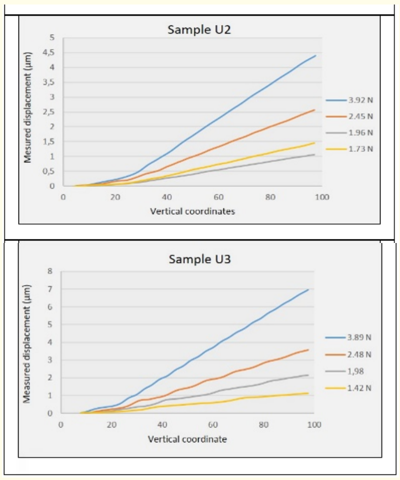

Figure 8a, 8b and 8c: Displacements measured with ESPI for the samples, U1, U2 and U3, with four different loads along the same profile.

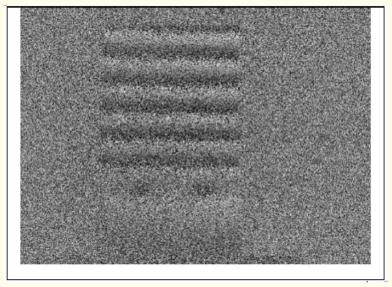

Figure 9a: Image of the phase map of the fringe pattern obtained for the sample U3 with a reaction force of 2.48 N.

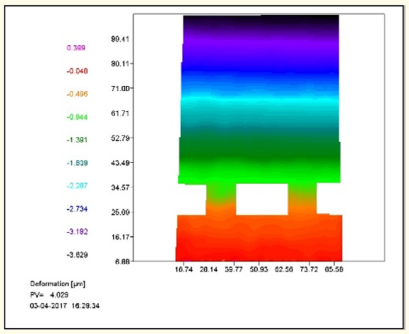

Figure 9b: Translation of the figure 9a into a colour code to allow a visual comparison with the FEA results shown on image 7.

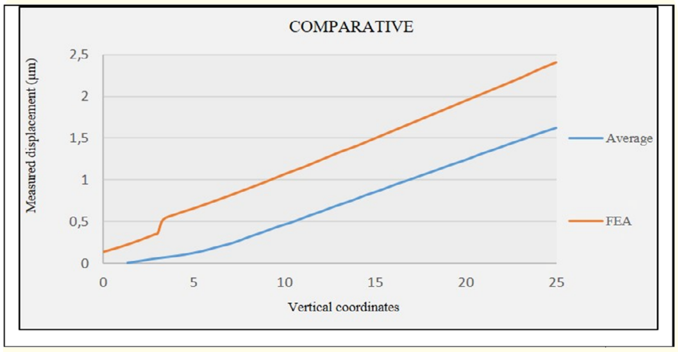

Figure 10: Comparative tendencies between the FEA results (orange) and the average calculated for the major reaction forces of the three samples (black). Despite the greater displacements measured on FEA, both lines exhibit the same tendency and a parallel behavior.

Discussion

As demonstrated by Eser., *et al*. [10] and Kim and co-workers [11], the expected validation of a numerical model has to consider the agreement of predictions enunciated by the FEA with the measured experimental results. It is not a matter of finding an exact quantitative coincidence but rather a similarity of tendencies and behaviors.

Comparing the obtained results, it is possible to observe that both, numerical and experimental models, exhibit a rotation displacement rather than a deformation, as well as the graphical findings related with the prosthetic framework geometrical characteristics, replicated for all the samples and all the reactions forces on ESPI. The representation of the results as a color code image put in evidence its similitude, highlighting the same behavior on both models.

U1			U2			U3		
1.66 N	Max	1,91222	1.73 N	Max	1,44729	1.42 N	Max	1,11652
	Min	0,00113		Min	0,00031		Min	0,02091
2.00 N	Max	3,69225	1,96 N	Max	1,06309	1.98 N	Max	2,13739
	Min	0,05475		Min	0,00199		Min	0,02614
2.36 N	Max	3,82458	2.45 N	Max	2,56583	2.48 N	Max	3,56038
	Min	0,0265		Min	0,0016		Min	0,00293
3.43 N	Max	6,67444	3.92 N	Max	4,39393	3.89 N	Max	6,96797
	Min	0,02386		Min	0,00595		Min	0,00953

Table 4: Maximum (Max) and minimum (Min) displacements measured for each sample and each reaction force, the values are presented in µm.

This similarity is also found by the direct comparison between the calculated average, considering the experimental models that showed the higher reaction forces, and the FEA, where the two lines define an angulation of 1, 09 degrees, representing a quite parallel behavior for both studies.

Experiments from Gröning., *et al.* [12,13], exploring the possibility of using optical methods to validate mathematical models, also found the same similarity of results. Likewise, Toro-Ibacache and co-workers [8] on the validation of a human cranial numerical model with a speckle interferometry approach, also found, despite the different magnitudes, similar strain distributions.

The quantitative differences may be explained by two different angles: On the one hand, all the simplifications and assumptions made during the FEA model preparation, such as the materials' properties and the friction coefficients, that although similar, were not the exact properties of the materials used on the experimental samples, the boundary conditions, that have a huge influence on determining the rotation center on the numerical model, could not be transported in an efficient way to the ESPI study, the geometrical simplifications on implants and implant screws could, as well, be of importance for the obtained results. On the other hand, must be considered the extreme sensibility of the ESPI method, where the signal-to-noise ratio could be low, mainly when low loads are applied, and the possibility of external factors disturb the results.

Conclusion

The described methodology and results allowed for the validation of a numerical model that intends to replicate a sort-implant screw-retained oral rehabilitation. Thus, within the limitations of the study, the validated model may be used to predict how different factors affect the mechanical behavior of such a rehabilitation. The use of different restorative materials in combination with different bone types, the study of how the occlusal scheme influences the stress generated on bone or on the prosthetic screws, or the testing of innovative prosthetic framework geometries may be analyzed combining different factors and levels. Such a wide variety of combinations would be undoable on clinical trials and would face possible ethical constrains.

The publication of more works on this field, describing the validation of oral rehabilitation models with optical techniques, namely speckle interferometry, would contribute to the establishment of more reproducible protocols and a more accurate knowledge of these methods by dental researchers.

Acknowledgments

Authors gratefully the funding of Project Norte-01-0145-FEDER-000022-SciTech-Science and Technology for Competitive and Sustainable Industries, cofinanced by Programa Operacional Regional do Norte (NORTE2020), through Fundo Europeu de Desenvolvimento Regional (FEDER).

Bibliography

1. J Nissan., *et al*. "The effect of crown/implant ratio and crown height space on stress distribution in unsplinted implant supporting restorations". *Journal of Oral and Maxillofacial Surgery* 69 (2011): 1934-1939.
2. Sütpideler M., *et al*. "Finite element analysis of effect of prosthesis height, angle of force application, and implant offset on supporting bone". *The International Journal of Oral and Maxillofacial Implants* 19 (2004): 819-825.
3. F Verri., *et al*. "Biomechanical influence of crown-to-implant ratio on stress distribution over internal hexagon short implant: 3-D finite element analysis with statistical test". *Journal of Biomechanics* 48 (2015): 138-145.
4. W Schulte. "Implants and the periodontium". *International Dental Journal* 45 (1995): 16-26.
5. Hämmerle CHF., *et al*. "Threshold of tactile sensitivity perceived with dental endosseous implants and natural teeth". *Clinical Oral Implants Research* 6.2 (1995): 83-90.
6. S Vidya Bhat., *et al*. "Stress Distribution Around Single Short Dental Implants: A Finite Element Study". *The Journal of the Indian Prosthodontic Society* 14 (2014): 161-167.
7. A Fayaz., *et al*. "Effects of Length and Inclination of Implants on Terminal Abutment Teeth and Implants in Mandibular CL1 Removable Partial Denture Assessed by Three-Dimensional Finite Element Analysis". *Journal of Dentistry* 12 (2015): 739-746.
8. V Toro-Ibacache., *et al*. "Validity and sensitivity of a human cranial finite element model: implications for comparative studies of biting performance". *Journal of Anatomy* 228 (2016): 70-84.
9. SA Wood., *et al*. "The effects of modeling simplifications on craniofacial finite element models: The alveoli (tooth sockets) and periodontal ligaments". *Journal of Biomechanics* 44 (2011): 1831-1838.
10. Eser A., *et al*. "Nonlinear finite element analysis versus ex vivo strain gauge measurements on immediately loaded implants". *The International Journal of Oral and Maxillofacial Implants* 24 (2009): 439-446.
11. Kim H-S., *et al*. "Finite element modeling technique for predicting mechanical behaviors on mandible bone during mastication". *The Journal of Advanced Prosthodontics* 4 (2012): 218-226.
12. F Gröning., *et al*. "Validating a voxel-based finite element model of a human mandible using digital speckle pattern interferometry". *Journal of Biomechanics* 42 (2009): 1224-1229.
13. F Gröning., *et al*. "The validation of finite element models with quantitative full-field strain comparisons". *Journal of Biomechanics* 45 (2012): 1498-1506.
14. Barak M., *et al*. "Optical metrology methods for mechanical testing of whole bones". *The Veterinary Journal* 180 (2009): 7-14.
15. Yap A., *et al*. "Non-destructive characterization of resin-based filling materials using Electronic Speckle Pattern Interferometry". *Dental Materials* 20 (2004): 377-382.
16. Ferreira J., *et al*. "7th Portuguese National Congress on Biomechanics". in Mechanical Performance of a short-implant supported oral fixed rehabilitation (a finite element analisys)". Minho University, Guimarães (2017).

Volume 2 Issue 12 December 2018